Microscopic approach to the scattering of unstable nuclei at intermediate incident energies

M. Yahiro[1]*, K. Ogata*[2]*, T. Matsumoto*[1] *and K. Minomo*[1]
[1]Department of Physics, Kyushu University, Fukuoka 812-8581, Japan
[2]Research Center for Nuclear Physics (RCNP), Osaka University, Osaka 567-0047, Japan

Abstract
This article presents the theoretical foundation of the continuum discretized coupled-channels method (CDCC). The validity of the Glauber model is also shown by extending the multiple scattering theory for nucleon-nucleus scattering to nucleus-nucleus scattering. The multiple scattering theory is applied to the scattering of unstable nuclei. This presentation is based on the recent review article on CDCC (arXiv:1203.5392[nucl-th]).

1 Introduction

Nuclear reaction is one of fundamental reactions in Nature and a good tool of understanding nucleon-nucleon (NN), nucleon-nucleus (NA) and nucleus-nucleus (AA) interactions and eventually structures of nuclei. One of the most important current subjects in nuclear physics is understanding of unstable nuclei. Unstable nuclei have exotic properties such as the halo structure [1–3] and the loss of magicity in the "island of inversion" [4–9]. The term "island of inversion" was introduced by Warburton [4] to the region of unstable nuclei from ^{30}Ne to ^{34}Mg. In the island of inversion, the first-excited states have low excitation energies and large $B(E2)$ values [5–9]. This indicates that the $N = 20$ magic number is not valid. anymore. These novel quantum properties have inspired a lot of works.

Important experimental tools of analyzing properties of unstable nuclei are the reaction cross section $\sigma_{\rm R}$ or the interaction cross section $\sigma_{\rm I}$ and the nucleon-removal cross section σ_{-n} [1–3, 10]. The experimental exploration of halo nuclei is moving from lighter nuclei such as He and C isotopes to relatively heavier nuclei such as Ne isotopes. Very lately $\sigma_{\rm I}$ was measured by Takechi *et al*. [11] for $^{28-32}$Ne located near or in the island of inversion. Furthermore, a halo structure of ^{31}Ne was reported by Nakamura *et al*. [12] with the experiment on σ_{-n}.

Understanding of unstable nuclei can be made by high-accuracy measurements and accurate theoretical analyses. The scattering of unstable nuclei have two features. The projectile is fragile and hence the projectile breakup is important. Measurements of the elastic scattering are not easy because of weak intensity of the secondary beam, and consequently, there is no reliable phenomenological optical potential. Therefore it is important to construct the microscopic reaction theory. This is a goal of the nuclear reaction theory.

A pioneering work on the microscopic description of NA scattering was done by Watson [13]. Kerman, McManus and Thaler (KMT) reformulated the multiple scattering theory as a series expansion in terms of an underlying NN t matrix [14]. The KMT theory was extended to AA scattering [15]. Another important microscopic model is the Glauber model [16]. This model is useful particularly for inclusive reactions. The theoretical foundation of the model can be obtained by the theory of Ref. 15. We show the details in Sec. 3.1. The Glauber model is based on the eikonal and the adiabatic approximation. The adiabatic approximation makes the breakup cross section diverge when the Coulomb interaction is included. Hence the Glauber model was mainly applied to lighter targets in which the Coulomb interaction is negligible. A way of making Coulomb corrections to the model has been proposed [17,18].

The continuum discretized coupled-channels method (CDCC) [19–21] is a fully quantum-mechanical method of treating the projectile breakup process in exclusive reactions such as elastic and inelastic scattering, elastic-breakup reactions and transferred reactions. The theoretical foundation of CDCC is shown

by clarifying the relation between the Faddeev method and CDCC [22–24]. We will show the detail in Sec. 2. Recent development and applications of CDCC are shown in Ref. [21].

The microscopic optical potential can be constructed by the g-matrix folding model [25–33]. For NA scattering, the folding model has succeeded in describing the elastic scattering systematically [32]. In general, the microscopic optical potential constructed is non-local, but it can be localized with the Brieva-Rook method [27]. The validity of this localization is shown in Ref. 34. For AA scattering at intermediate and high incident energies, the folding model is also successful in describing the scattering, since the projectile breakup is weak. This is discussed in Sec. 3. One can use the microscopic optical potential as an input of CDCC calculations.

2 Theoretical foundation

Following Refs. 22–24, We consider the projectile (P) that is composed of two particles b and c. In this case, the scattering of P on a target (A) can be described by the A+b+c three-body system. The three-body scattering is governed by the three-body Schrödinger equation

$$[H - E]\Psi = 0 \tag{1}$$

with the Hamiltonian

$$H = K_r + K_R + v(\mathbf{r}) + U_b(\mathbf{r}_b) + U_c(\mathbf{r}_c), \tag{2}$$

where K_r and K_R are the kinetic energy operators associated with the relative coordinate $\mathbf{r}$ between b and c and the relative coordinate $\mathbf{R}$ between P and A, respectively, and $v(\mathbf{r})$ is the interaction between b and c, while U_b (U_c) is an optical potential between b (c) on A.

In CDCC, the total wave function Ψ is expanded in terms of the complete set of eigenfunctions of Hamiltonian $h = K_r + v(\mathbf{r})$ [19,20]. The eigenfunctions consist of bound and continuum states. The continuum states are characterized by orbital angular momentum ℓ and linear momentum k of the b+c subsystem. They are truncated as

$$k \le k_{\max}, \quad \ell \le \ell_{\max}. \tag{3}$$

After making the truncations, we further discretize the k contiuum. Hence the modelspace $\mathcal{P}'$ is described as

$$\mathcal{P}' = \sum_{i=0}^{N} |\phi_i\rangle\langle\phi_i|, \tag{4}$$

where the ϕ_i represent the bound and discretized-continuum states of h and N is the number of the ϕ_i. The total wave function Ψ is hence approximated into

$$\Psi \approx \Psi_{\rm CDCC} \equiv \mathcal{P}'\Psi = \sum_{i=0}^{N} \phi_i(\boldsymbol{r})\chi_i(\boldsymbol{R}), \tag{5}$$

where the coefficient $\chi_i(\boldsymbol{R})$ describes a motion of P in its state ϕ_i. The approximate total wave function $\Psi_{\rm CDCC}$ is obtained by solving the three-body Schrödinger equation (1) in the modelspace $\mathcal{P}'$:

$$\mathcal{P}'[H - E]\mathcal{P}'\Psi_{\rm CDCC} = 0. \tag{6}$$

The S-matrix elements calculated with CDCC depend on the size of the modelspace P'. This artifact should be removed by confirming that the calculated S-matrix elements converge as the modelspace is enlarged. Actually the convergence was first shown in Refs. 19,20,35. The next question to be addressed is whether the converged S-matrix elements are exact.

CDCC is based on three approximations, the ℓ-truncation, the k-truncation and the discretization of k-continuum. The ℓ-truncation is most essential among these approximations, as shown below. Now we introduce the projection operator $\mathcal{P}$ that only selects ℓ up to $\ell_{\max}$. Obviously, $\mathcal{P}'$ tends to $\mathcal{P}$ in the limit of large $k_{\max}$ and small width of momentum bin. The component $\mathcal{P}\Psi$ has no asymptotic amplitudes in the rearrangement channels. For example, let us consider a simple case of $\ell_{\max} = 0$. In this case, $\mathcal{P}U\mathcal{P}$ is the average of $U = U_b + U_c$ over the angle of vector $\mathbf{r}$. Hence the potential $\mathcal{P}U\mathcal{P}$ becomes a function of r and R. Thus $\mathcal{P}U\mathcal{P}$ is a three-body potential that vanishes at large R and/or large r, so that it does not generate any rearrangement channel.

The insertion of three-body distorting potentials does not change the mathematical properties of the Faddeev equations [36]. Now we consider $\mathcal{P}U\mathcal{P}$ as such a distorting potential in order to obtain the distorted Faddeev equations,

$$(E - K_r - K_R - v - \mathcal{P}U\mathcal{P})\psi_A = v(\psi_b + \psi_c), \tag{7}$$

$$(E - K_r - K_R - U_b)\psi_b = (U_b - \mathcal{P}U_b\mathcal{P})\psi_A + U_b\psi_c, \tag{8}$$

$$(E - K_r - K_R - U_c)\psi_c = (U_c - \mathcal{P}U_c\mathcal{P})\psi_A + U_c\psi_b, \tag{9}$$

where ψ_A, ψ_b and ψ_c satisfy the relation $\Psi = \psi_A + \psi_b + \psi_c$. If Eqs. (7)-(9) are added, the original three-body Schrödinger equqtion (1) is recovered. In an iterative approach to Eqs. (7)-(9), the zeroth order solution for ψ_A is obtained by setting the right-hand side of (7) to zero. The zeroth order solution is nothing but $\Psi_{\rm CDCC}$. When $\Psi_{\rm CDCC}$ is inserted in Eqs. (8)-(9), the equations do not generate any disconnected diagram, since $\Psi_{\rm CDCC}$ has no rearrangement channel in the asymptotic region. Furthermore, the subtractions, $U_b - \mathcal{P}U_b\mathcal{P}$ and $U_c - \mathcal{P}U_c\mathcal{P}$, sizably weaken couplings of $\Psi_{\rm CDCC}$ with ψ_b and ψ_c. Thus $\Psi_{\rm CDCC}$ is a good solution to the three-body Schrödinger equation (1), when $\ell_{\max}$ is large enough. Very lately, the CDCC solution was compared with the Faddeev solution through numerical calculations. The two solutions agree with each other [24].

3 Microscopic reaction theory for AA scattering

The most fundamental equation to describe AA scattering is the many-body Schrödinger equation with the realistic NN interaction v_{ij}:

$$(K + h_{\rm P} + h_{\rm T} + \sum_{i\in{\rm P}, j\in{\rm T}} v_{ij} - E)\hat{\Psi}^{(+)} = 0\,, \tag{10}$$

where K is the kinetic-energy operator for the relative motion between P and T and $h_{\rm P}$ ($h_{\rm A}$) is the internal Hamiltonian of P (T). The scattering of P from T can be described with a series of multiple scattering in terms of v_{ij}. In the series, one can first take a summation of ladder diagrams between the same NN pair. The summation can be described by an effective NN interaction τ_{ij} in nuclear medium. Taking a resummation of the series in terms of τ_{ij}, one can get the many-body Schrödinger equation with τ_{ij} [15]:

$$(K + h_{\rm P} + h_{\rm T} + \sum_{i\in{\rm P}, j\in{\rm T}} \tau_{ij} - E)\hat{\Psi}^{(+)} = 0\,. \tag{11}$$

Here the number of v_{ij} between P and T is assumed to be much larger than 1 and the antisymmetrization between incident nucleons in P and target nucleons in T can be approximated by using τ_{ij} that is properly symmetrical with respect to the exchange of the colliding nucleons. The first assumption is good for AA scattering, and the second one is known to be accurate at intermediate and high incident energies [37,38]. This theory of Ref. 15 is an extension of the KMT theory [14] for NA scattering to AA scattering.

Since τ_{ij} describes NN scattering in nuclear medium, the Brueckner g-matrix is commonly used as τ_{ij} in many applications; see for example Refs. 25–33. The g-matrix interaction does not include any effect induced by finite nucleus, e.g. effects of target collective excitations, because the interaction is evaluated in infinite nuclear matter.

3.1 Validity of the Glauber model

We show the validity of the Glauber model by using the many-body Schrödinger equation (11) with the effective NN interaction, following Ref. 15. The Glauber model is based on the eikonal approximation for NN scattering and the eikonal and adiabatic approximations for AA scattering. The condition for the eikonal approximation to be good for NN collision in both free space and AA scattering is that

$$|v(\boldsymbol{r})/e| \ll 1, \quad ka \gg 1\ , \tag{12}$$

where e (k) is a kinetic energy (wave number) of NN collision, $\boldsymbol{r}$ is the relative coordinate between two nucleons and a is a range of the realistic NN interaction v. This condition is not well satisfied for the realistic NN potential that has a strong short-ranged repulsive core; for example, $v \sim 2000$ MeV at $r = 0$ for AV18 [39]. In fact, the eikonal approximation is not good for NN scattering at intermediate energies, as shown in the left panel of Fig. 1. To avoid this problem, a slowly-varying function such as the Gaussian form has been used as a profile function in the Glauber model [40].

The usage of slowly-varying profile function and hence of slowing-varying NN interaction can be justified by using the many-body Schrödinger equation (11). Applying the adiabtic and eikonal approximations to Eq. (11), one can obtain the S-matrix of AA scattering as

$$S = \exp\Big[-\frac{i}{\hbar v_{\rm rel}} \sum_{ij} \int_{-\infty}^{\infty} dz_{ij} \tau_{ij} \Big], \tag{13}$$

where $v_{\rm rel}$ stands for a velocity of P relative to A and z_{ij} is the z-component of the relative coordinate $\boldsymbol{r}_{ij}$ between two nucleons. In general, τ_{ij} has much milder r dependence than the bare NN potential v_{ij} [15]. In the case of large incident energies, for instance, τ_{ij} is reduced to the t-matrix of NN scattering that is a product of v_{ij} and the wave operator of NN scattering. When v_{ij} has a strong repulsive core at small r, the wave operator is largely suppressed there. This leads to the fact that the t matrix is a slowly-varying function of r [15]. The g matrix [26] proposed by Jeukenne, Lejeune and Mahaux (JLM) keeps this property. The g matrix is thus more suitable than v_{ij} as an input of the Glauber model. In fact, as shown in the right panel of Fig. 1, the eikonal approximation is quite good for NN scattering at intermediate energies, say 150 MeV, when the JLM g matrix is used. The usage of the g-matrix interaction has another merit in the sense that the effective interaction includes nuclear medium effects.

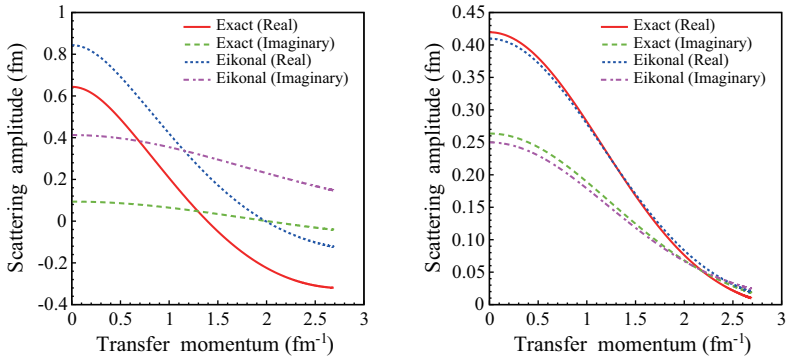

Fig. 1: (Color online) The on-shell NN scattering amplitude $f_{\rm NN}(\boldsymbol{q})$ at the laboratory energy $E_{\rm NN} = 150$ MeV calculated with the bare NN potential AV18 in the left panel and with the JLM g matrix [26] in the right panel. The solid (dashed) and dotted (dash-dotted) lines show, respectively, the real and imaginary parts of $f_{\rm NN}(\boldsymbol{q})$ of the exact (eikonal) calculation.

3.2 Application of the g-matrix folding model to AA scattering

Following Refs. 41–43, we consider two types of effective NN interactions in the folding model: the Love-Franey t-matrix interaction ($t_{\rm LF}$) [44], and the Melbourne interaction ($g_{\rm MB}$) [32] constructed from the Bonn-B realistic NN interaction [45]. For stable nuclei, we take the phenomenological proton-density [46] deduced from the electron scattering by unfolding the finite-size effect of the proton charge. The neutron density is assumed to have the same geometry as the corresponding proton one, since in the present case the proton RMS radius deviates from the neutron one only by less than 1% in the Hartree-Fock (HF) calculation. For Ne isotopes, the densities are constructed by antisymmetrized molecular dynamics (AMD) [47] with the Gogny D1S interaction [48,49]

Figure 2 shows the results of the g- and t-matrix folding models for the angular distribution of ^{12}C+^{12}C elastic scattering at 135 MeV/nucleon in the left panel and 74.25 MeV in the right panel. In the left panel, the g-matrix folding model (solid line) well reproduces the data [50] with no free parameter, whereas the t-matrix folding model (dashed line) does not. Also for the low incident energy in the right panel, the g-matrix folding model (solid line) yields better agreement with the data [51] than the t-matrix folding model (dashed line). For scattering angles larger than 50 degree, the solid line does not reproduce the data perfectly. The deviation may come from effects of collective projectile and target excitations that are not included in the g-matrix. The g-matrix folding model is thus quite reliable particularly for intermediate incident energies.

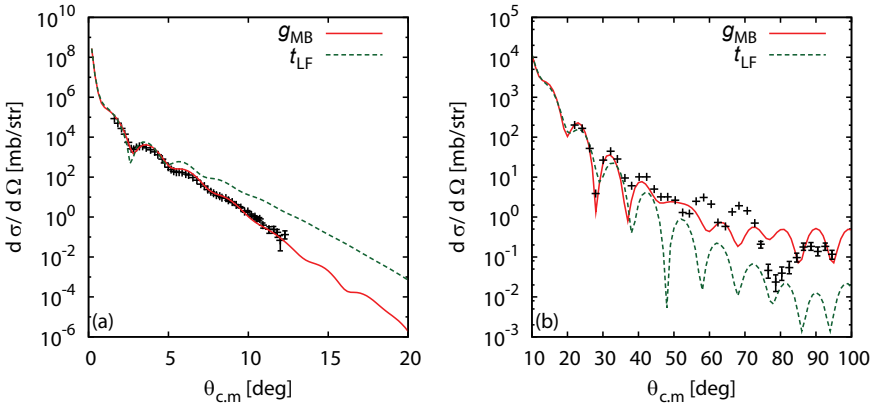

Fig. 2: (Color online) Angular distributions of ^{12}C+^{12}C elastic cross sections at 135 MeV/nucleon in the left panel and 74.25 MeV in the right panel. The solid (dashed) line stands for the results of DFM calculations with $g_{\rm MB}$ ($t_{\rm LF}$). The data is taken from Ref. [50] in the left panel and from Ref. [51] in the right panel.

The left panel of Fig. 3 shows the reaction cross sections for the scattering of ^{12}C from ^{12}C, ^{20}Ne, ^{23}Na, and ^{27}Al targets. The dotted and solid lines represent results of the g-folding calculations before and after the normalization with $F = 0.978$, respectively. Before the normalization procedure, the dotted line slightly overestimates the mean values of data for $A = 20$–27. After the normalization procedure, the solid line agrees with the mean values of data for all the targets. The normalization procedure is thus reliable. The dashed line corresponds to the results of the t-folding calculations with no normalization. The medium effect reduces the theoretical reaction cross sections by about 15% for all the targets.

The right panel of Fig. 3 represents $\sigma_{\rm R}$ for $^{20-32}$Ne + ^{12}C systems at 240 MeV/nucleon. The g-matrix folding model with the AMD density (solid line) reproduces the data [11], whereas the spherical Hatree-Fock (HF) calculation with the Gogny D1S interaction (dotted line) underestimates the data. It

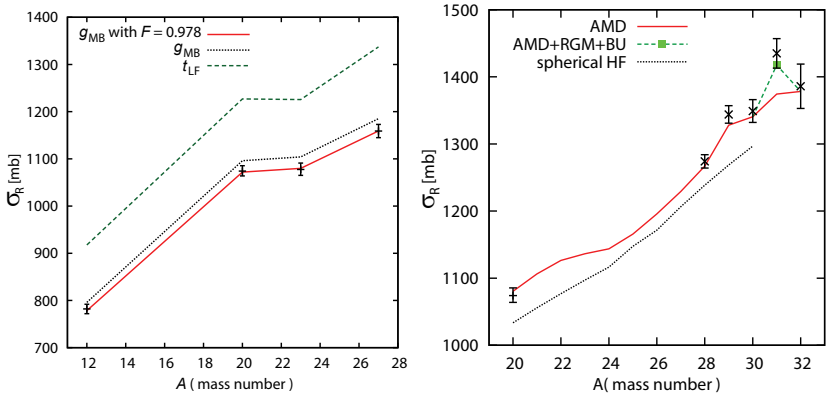

Fig. 3: (Color online) Reaction cross sections for the scattering of ^{12}C on stable nuclei from $A = 12$ to 27 in the left panel and for the scattering of Ne isotopes from a ^{12}C target at 240 MeV/nucleon in the right panel. In the left panel, the data at 250.8 MeV/nucleon for ^{12}C and ^{27}Al are taken from Ref. [52]. The data at 240 MeV/nucleon for ^{20}Ne and ^{23}Na are deduced from measured σ_I at around 1 GeV/nucleon [53,54] with the Glauber model [11]. The solid (dotted) line stands for the results of the g-matrix folding model after (before) the normalization with $F = 0.978$, whereas the dashed line corresponds to results of the t-matrix folding model. In the right panel, the solid (dotted) line represents the results of AMD (spherical HF) calculations. The dashed line with a closed square is the result of the AMD calculation with the tail and breakup corrections. The closed square represents the result of the AMD+RGM calculation with breakup correction. The experimental data for $A = 28 - 32$ are taken from Ref. 11.

should be noted that the nuclei with $A > 30$ are unbound in the spherical calculations, where A is the mass number of P. The enhancement from the dotted line to the solid line stems from the deformation of P. The g-matrix folding model with the AMD density thus yields results consistent with the data except ^{31}Ne. The underestimation of this model for ^{31}Ne comes from the inaccuracy of the AMD density in its tail region.

The tail correction to the AMD density can be made as below. The ground state of ^{31}Ne is described by the ^{30}Ne+n cluster model with excitations of ^{30}Ne. The cluster-model calculation can be done with the resonating group method (RGM) in which the ground and excited states of ^{30}Ne are constructed with AMD. This AMD+RGM calculation is quite time consuming, but it is done for ^{31}Ne. The tail correction to σ_R is 35 mb. The reaction cross section with the tail correction (a square symbol) well reproduces the experimental data [11] with no adjustable parameter. Consequently, ^{31}Ne is a halo nucleus with large deformation.

4 Summary

We have shown recent developments of CDCC and the microscopic reaction theory as an underlying theory of CDCC. This talk is based on the recent review article of Ref. 21.

First we have shown the theoretical foundation of CDCC by comparing the Faddeev method and CDCC. The primary approximation in CDCC is the ℓ-truncation P. The ℓ-truncation changes the two-body potentials, U_b and U_c, to three-body ones. The theoretical foundation of the ℓ-truncation is investigated with the distorted Faddeev equations where the three-body potentials $\mathcal{P}U_b\mathcal{P}$ and $\mathcal{P}U_c\mathcal{P}$ are inserted. The CDCC solution is the zeroth-order solution to the distorted Faddeev equations. The first-order solution is strongly weakened by the suppression of coupling potentials, $U_b - \mathcal{P}U_b\mathcal{P}$ and $U_c - \mathcal{P}U_c\mathcal{P}$.

The CDCC solution is thus a good solution to the three-body Schrödinger equation, when $\ell_{\max}$ is large enough. The theoretical statement based on the distorted Faddeev equations is numerically confirmed to be true by a direct comparison between the CDCC and Faddeev solutions [24].

As an underlying theory of CDCC, we have constructed a microscopic reaction theory for AA scattering, using the multiple scattering theory. This is an extension of the KMT theory for nucleon-nucleus scattering to nucleus-nucleus scattering. The input of the theory is the g-matrix NN interaction instead of the realistic one. The g-matrix has much milder r-dependence, so that the Glauber model becomes reliable when the model starts from the microscopic reaction theory of Ref. 15. The Glauber model is applicable for the scattering of lighter projectiles from lighter targets at intermediate and high incident energies, since Coulomb breakup is weak there.

Using the g-matrix folding model, one can construct the microscopic optical potential with projectile and target densities calculated by fully microscopic structure theories such as AMD and HF. This fully microscopic framework has been applied to the scattering of stable nuclei and unstable neutron-rich Ne-isotopes at intermediate incident energies with success of reproducing the data. In "the Island of inversion" region, the nuclei are strongly deformed, and ^{31}Ne is a halo nucleus with strong deformation. The reliable microscopic optical potential can be used as an input of CDCC calculations. This microscopic version of CDCC is quite useful to analyze the scattering of unstable nuclei.

References

[1] I. Tanihata, *et al*., Phys. Lett. B **289**, 261 (1992).
I. Tanihata, J. Phys. G **22**, 157 (1996).

[2] A. S. Jensen, *et al*., Rev. Mod. Phys. **76**, 215 (2004).

[3] B. Jonson, Phys. Rep. **389**, 1 (2004).

[4] E. K. Warburton, J. A. Becker, and B. A. Brown, Phys. Rev. C **41**, 1147 (1990).

[5] T. Motobayashi *et al*., Phys. Lett. B **346**, 9 (1995).

[6] E. Caurier, F. Nowacki, A. Poves, J. Retamosa, Phys. Rev. C **58**, 2033 (1998).

[7] Y. Utsuno, T. Otsuka, T. Mizusaki, M. Honma, Phys. Rev. C **60**, 054315 (1999).

[8] H. Iwasaki *et al*., Phys. Lett. B **522**, 227 (2001).

[9] Y. Yanagisawa *et al*., Phys. Lett. B **566**, 84 (2003).

[10] A. Gade, *et al*., Phys. Rev. C **77**, 044306 (2008).

[11] M. Takechi *et al*., Nucl. Phys. **A834**, 412c (2010).

[12] T. Nakamura, *et al*., Phys. Rev. Lett. **103**, 262501 (2009).

[13] K. M. Watson, Phys. Rev. **89**, 575 (1953).

[14] A. K. Kerman, H. McManus, and A. M. Thaler, Ann. Phys.(N.Y.) 8, **51** (1959).

[15] M. Yahiro, K. Minomo, K. Ogata, and M. Kawai, Prog. Theor. Phys. **120**, 767 (2008).

[16] R.J. Glauber, *in Lectures in Theoretical Physics* (Interscience, New York, 1959), Vol. 1, p.315.

[17] B. Abu-Ibrahim and Y. Suzuki, Prog. Theor. Phys. **112** (2004), 1013; B. Abu-Ibrahim and Y. Suzuki, Prog. Theor. Phys. **114** (2005), 901.

[18] P. Capel, D. Baye, and Y. Suzuki, Phys. Rev. C **78** (2008), 054602.

[19] M. Kamimura, M. Yahiro, Y. Iseri, Y. Sakuragi, H. Kameyama and M. Kawai, Prog. Theor. Phys. Suppl. **89** (1986), 1.

[20] N. Austern, Y. Iseri, M. Kamimura, M. Kawai, G. Rawitscher and M. Yahiro, Phys. Rep. **154** (1987), 125.

[21] M. Yahiro, K. Ogata, T. Matsumoto and K. Minomo, Prog. Theory. Exp. Phys. **1** (2012), 01A209 [arXiv:1203.5392 [nucl-th]].

[22] N. Austern, M. Yahiro, and M. Kawai, Phys. Rev. Lett. **63** (1989), 2649.

[23] N. Austern, M. Kawai, and M. Yahiro, Phys. Rev. C **53** (1996), 314.
[24] A. Deltuva, A.M. Moro, E. Cravo, F.M. Nunes, and A.C. Fonseca, Phys. Rev. C **76** (2007), 064602.
[25] G. Bertsch, J. Borysowicz, M. McManus, and W.G. Love, Nucl. Phys. A**284**, 399(1977).
[26] J.-P. Jeukenne, A. Lejeune and C. Mahaux, Phys. Rev. C**16**, 80 (1977); ibid. Phys. Rep. **25**, 83 (1976).
[27] F.A. Brieva and J.R. Rook, Nucl. Phys. A**291**, 299 (1977); ibid. 291, 317 (1977); ibid. 297, 206 (1978).
[28] G. R. Satchler, Phys. Rep. **55**, 183-254 (1979).
[29] G. R. Satchler, "Direct Nuclear Reactions", Oxfrod University Press, (1983).
[30] N. Yamaguchi, S. Nagata and T. Matsuda, Prog. Theor. Phys. **70**, 459 (1983); N. Yamaguchi, S. Nagata and J. Michiyama, Prog. Theor. Phys. **76**, 1289 (1986).
[31] L. Rikus, K. Nakano and H. V. von Geramb, Nucl. Phys. A**414**, 413 (1984); L. Rikus and H.V. von Geramb, Nucl. Phys. A**426**, 496 (1984).
[32] K. Amos, P. J. Dortmans, H. V. von Geramb, S. Karataglidis, and J. Raynal, in *Advances in Nuclear Physics*, edited by J. W. Negele and E. Vogt(Plenum, New York, 2000) Vol. 25, p. 275.
[33] T. Furumoto, Y. Sakuragi, and Y. Yamamoto, Phys. Rev. C**78**, 044610 (2008); *ibid*., C**79**, 011601(R) (2009); *ibid*., C**80**, 044614 (2009).
[34] K. Minomo, K. Ogata, M. Kohno, Y. R. Shimizu and M. Yahiro, J. Phys. G **37**, 085011 (2010) [arXiv:0911.1184 [nucl-th]].
[35] R. A. D. Piyadasa, M. Kawai, M. Kamimura and M. Yahiro, Phys. Rev. C **60**, 044611(1999); R. A.D. Piyadasa, M. Yahiro, M. Kamimura and M. Kawai, Prog. Theor. Phys. **81**, 910 (1989).
[36] M.C. Birse and E. F. Redish, Nucl. Phys. A**406**, 149.
[37] G. Takeda and K. M. Watson, Phys. Rev. **97**, 1336(1955).
[38] A. Picklesimer and R. M. Thaler, Phys. Rev. C**23**, 42(1981).
[39] R. B. Wiringa, V. G. J. Stoks and R. Schiavilla, Phys. Rev. C**51**, 38 (1995).
[40] R.J. Glauber and G. Matthiae, Nucl. Phys. B**21**, 135 (1970).
[41] K. Minomo, T. Sumi, M. Kimura, K. Ogata, Y. R. Shimizu, and M. Yahiro, Phys. Rev. C **84**, 034602 (2011).
[42] K. Minomo, T. Sumi, M. Kimura, K. Ogata, Y. R. Shimizu and M. Yahiro, Phys. Rev. Lett. **108** (2012), 052503.
[43] T. Sumi *et al*., Phys. Rev. C **85** (2012), 064613.
[44] W. G. Love and M. A. Franey, Phys. Rev. C**24**, 1073 (1981); M. A. Franey and W. G. Love, Phys. Rev. C**31**, 488 (1985).
[45] R. Machleidt, K. Holinde, and Ch. Elster, Phys. Rep. **149**, 1(1987).
[46] H. de Vries, C. W. de Jager, and C. de Vries, At. Data Nucl. Data Tables **36**, 495 (1987).
[47] M. Kimura and H. Horiuchi, Prog. Theor. Phys. 111, 841 (2004); M. Kimura, Phys. Rev. C 75, 041302 (2007). M. Kimura, arXiv:1105.3281 (2011) [nucl-th].
[48] J. Decharge and D. Gogny, Phys. Rev. C **21** (1980), 1568.
[49] J. F. Berger, M. Girod, and D. Gogny, Comp. Phys. Comm. **63** (1991), 1365.
[50] T. Ichihara *et al*., Nucl. Phys. A**569** 287c-296c(1994).
[51] R. G. Stokstad, *et al*., Phys. Rev. C **20**, 655 (1979).
[52] M. Takechi, *et al*., Phys. Rev. C **79**, 061601(R) (2009).
[53] T. Suzuki *et al*., Phys. Rev. Lett. **75**, 3241 (1995).
[54] L. Chulkov *et al*., Nucl. Phys. **A603** 219, (1996).